Published in Acta Materialia, vol.57(6), pp. 2010-2019 (2009)

Thermoelectric properties of ternary and Al-containing quaternary $Ru_{1-x}Re_xSi_y$ chimney-ladder compounds

Kyosuke Kishida, Akira Ishida, Tatsuya Koyama, Shunta Harada, Norihiko L. Okamoto, Katsushi Tanaka, and Haruyuki Inui

Department of Materials Science and Engineering, Kyoto University
Sakyo-ku, Kyoto 606-8501, JAPAN

ABSTRACT

Thermoelectric properties of ternary and Al-containing quaternary $Ru_{1-x}Re_xSi_y$ chimney-ladder phases have been studied as a function of the Re concentration with the use of directionally solidified alloys. The $Ru_{1-x}Re_xSi_y$ chimney-ladder phases exhibit n- and p-type semiconducting behaviors respectively at low and high Re concentrations, at which the X(=Si)/M(=Ru+Re) ratios are respectively, larger and smaller than those expected from the VEC (valence electron concentration)=14 rule. The absolute values of both Seebeck coefficient and electrical resistivity increase as the extent of the deviation from the VEC=14 rule increases, i.e., as the alloy composition deviates from that corresponding to the p-n transition ($x \approx 0.5$), indicating that the carrier concentration can be controlled by changing the extent of compositional deviation from the ideal VEC=14 composition. The highest values of dimensionless figure of merit obtained are 0.47 for ternary (x = 0.60) and 0.56 for Al-containing quaternary alloys. The reasons for the systematic compositional deviation from the ideal VEC=14 compositions observed for a series of chimney-ladder phases are discussed in terms of atomic packing.

Keywords: transition metal silicides; thermoelectric; crystal structure; electron diffraction; semiconductor compounds

* Corresponding author. : Kyosuke Kishida
Department of Materials Science and Engineering,
Kyoto University, Sakyo-ku, Kyoto 606-8501, JAPAN
E-mail address: k.kishida@materials.mbox.media.kyoto-u.ac.jp
Tel.: +81-75-753-5481; fax: +81-75-753-5461

1. INTRODUCTION

Ruthenium sesquisilicide Ru_2Si_3 has been considered as a promising candidate for a high-temperature thermoelectric material because of its high Seebeck coefficient and low thermal conductivity [1-14]. Ru_2Si_3 crystallizes into two different types of structures; the tetragonal-type high-temperature (HT) phase and the orthorhombic-type low-temperature (LT) phase [15]. The HT-Ru_2Si_3 phase is a member of a family of materials known as Nowotny "chimney-ladder" phases [15]. The chimney-ladder phase generally formulated to be M_nX_{2n-m} has a structure composed of subcells of transition metal (M) atoms in a tetragonal β-Sn arrangement ("chimney") and group 14 or 13 atoms (X) in a coupled helical arrangement ("ladder"), with both the chimney and ladder being aligned along the c-axis of the tetragonal unit cell, where n and m indicate, respectively, the numbers of M and X subsells in the unit cell of a given chimney-ladder phase [16-20]. Extensive studies on various chimney-ladder phases have revealed that most chimney-ladder phases tend to satisfy a valence electron concentration rule, i.e. they are stabilized when the valence electron concentration per transition-metal atom (VEC) is equal to 14. Under this circumstance, the Fermi energy of the chimney-ladder phases is located in a middle of a narrow band gap so that they exhibit semiconducting properties [7,19-21]. The semiconducting nature together with low thermal conductivity originating from the complex crystal structure makes the chimney-ladder phases including HT-Ru_2Si_3 attractive as a possible thermoelectric material [3].

Since the chimney-ladder phases are electron compounds following the valence electron concentration rule (VEC=14), the crystal structure and therefore the intrinsic physical properties are expected to be controlled by alloying with a substitutional element, especially when the number of valence electrons of the alloying element is different from that of the constituent element [16-20]. Recently, we have studied the phase relationship in the Ru-Re-Si systems using polycrystalline samples produced by arc-melting and found that the HT-Ru_2Si_3 phase with the chimney-ladder structure is stabilized to appear at low temperatures by the partial substitution of Ru atoms (group 8) with Re atoms (group 7) [11]. A series of $Ru_{1-x}Re_xSi_y$ chimney-ladder phases exists roughly along the composition line connecting two end binary phases satisfying the VEC=14 rule, namely Ru_2Si_3 and Re_4Si_7, in the Ru-Re-Si ternary phase diagram over a wide compositional range of $0.14 \leq x \leq 0.76$. However, the observed x-y relation for the $Ru_{1-x}Re_xSi_y$ chimney-ladder phase was found to deviate systematically from the relation expected from the VEC=14 rule, i.e. $y = 1.5 + 0.25x$. The actual composition line was determined to be $y = 1.539 + 0.178x$ ($Ru_{1-x}Re_xSi_{1.539+0.178x}$) [11]. The compositional deviation from the composition satisfying the VEC = 14 rule is expected to be used to predict the semiconducting properties of the chimney-ladder phases, when referring to the calculation by Imai and Watanabe [22], and Migas et al. [21]. The compositional deviation from the VEC=14 rule for Re-poor $Ru_{1-x}Re_xSi_y$ chimney-ladder phases occurs in a way that there exist more Si atoms than the VEC=14 rule predicts so that these chimney-ladder phases exhibit the n-type conducting behavior due to the existence of additional electrons [11]. On the other hand, the compositional deviation from the VEC=14 rule for Re-rich $Ru_{1-x}Re_xSi_y$ chimney-ladder phases occurs in a way that there exist less Si atoms than the VEC=14 rule predicts so that these chimney-ladder phases exhibit the p-type conducting behavior [11]. The p-n transition is predicted to occur at $x \approx 0.5$ from the change in the sign of the compositional deviation from the VEC=14 rule. Our preliminary measurement of Seebeck coefficient with the use of polycrystalline alloys has indeed indicated that $Ru_{1-x}Re_xSi_y$ chimney-ladder phases actually exhibit n-type and p-type semiconducting behaviors when the alloy compositions are Re-poor and Re-rich, respectively [11]. However, since the extent of the compositional

variation in the chimney-ladder phases observed in the polycrystalline specimens produced by arc-melting is quite large (the difference in the Re content in chimney-ladder phases for a given specimen is usually as large as 15-20%), the exact composition for the p-n transition has not yet been experimentally confirmed. This has to be clarified with specimens with less compositional variation in the chimney-ladder phases. On top of that, to establish a way to control the compositional deviation from the composition satisfying the VEC=14 rule is a key factor to provide the chimney-ladder phases with desirable thermoelectric properties through not only changing the type of carrier but also their concentrations. It is thus quite important to elucidate the origin of the compositional deviation from the ideal value satisfying the VEC=14 rule. Although many studies on some chimney-ladder phases have been carried out so far to explain the reason why they are formed so as to maintain the VEC=14 rule [19,20,23], the reasons for the compositional deviation observed for most of the chimney-ladder phases, especially when large amounts of substitutions are made, have not been studied in details.

In the present study, we investigate the thermoelectric properties of the $Ru_{1-x}Re_xSi_y$ chimney-ladder phases as a function of the Re content (x in $Ru_{1-x}Re_xSi_y$), i.e., as a function of the sign and amount of compositional deviation from the ideal value satisfying the VEC = 14 rule, with the use of directionally solidified alloys for which less compositional variations are expected to occur in the chimney-ladder phases, in order to get insight into the reasons for the compositional deviation. We also investigate the effects of Al additions on the thermoelectric properties and the compositional deviation of $Ru_{1-x}Re_xSi_y$ chimney-ladder phases, in order to see whether the compositional deviation from the ideal value satisfying the VEC=14 rule, thereby their physical properties can be further controlled by quaternary alloying.

2. EXPERIMENTAL PROCEDURE

Rod ingots of ternary $Ru_{1-x}Re_xSi_{1.54+0.18x}$ alloys with x = 0.14, 0.23, 0.36, 0.53, 0.60, and 0.73 and quaternary $Ru_{0.27}Re_{0.73}(Si_{1-\delta}Al_\delta)_{1.67}$ alloys with δ = 0.04, 0.08 and 0.16 were produced by arc-melting elemental Ru (3N-grade), Re (4N-grade), semiconductor-grade Si and Al (4N-grade) in an Ar atmosphere. For Al-substituted alloys, the Re/M ratio is fixed at 0.73, which is close to the solubility limit of Re in the chimney-ladder phases of the Ru-Re-Si ternary system. These ingots were directionally solidified in an optical floating zone (FZ) furnace at a growth rate of 5.0 mm/h. Microstructures of as-grown crystals were examined by scanning electron microscopy (SEM) and transmission electron microscopy (TEM). Chemical compositions for selected regions of interest in as-grown crystals were estimated by energy dispersive x-ray spectroscopy (EDS) in SEM and TEM. The Al/Si ratios for the Al-substituted samples were estimated by wavelength dispersive X-ray spectroscopy (WDS). Lattice constants of the metal sublattice of chimney-ladder phases were examined by powder X-ray diffraction (XRD). Specimens for TEM observations were prepared by mechanical polishing, dimple grinding and finally Ar-ion milling at 4 kV for electron transparency.

Rectangular specimens with the approximate dimensions of 2 × 2 × 7 mm^3 were cut from directionally solidified ingots by electric discharge machining for measurements of Seebeck coefficient and electrical resistivity. Measurements of Seebeck coefficient and electrical resistivity were made with our ULVAC ZEM-2 apparatus in the temperature range from 173 K to 973 K at an interval of 50 K with measurement errors of less than ±7% and ±10%, respectively. Values of thermal conductivity were estimated from those of thermal diffusivity and specific heat measured by the laser flash method with our ULVAC TC-7000 apparatus for thin-disc specimens with a diameter of 8 mm and a thickness of 1 mm in the

temperature range from room temperature to 973 K at an interval of 100 K. It should be noted that values of the thermal conductivity estimated by this method generally contains an experimental error less than ±10%.

3. RESULTS

3.1. Directional solidified ingots

Fig. 1 shows SEM backscattered electron (BSE) images of directionally solidified $Ru_{1-x}Re_xSi_{1.54+0.18x}$ ternary alloys with nominal alloy compositions of x = 0.36 and 0.60 observed in a cross section cut parallel and perpendicular to the growth direction. Although no additional phases are observed in all directionally solidified ternary alloys, fine regions with slightly different brightness are observed within a region having chemical compositions corresponding to the chimney-ladder phases. EDS analysis in a SEM has revealed that the brightness differences correspond to compositional variation in the chimney-ladder phases (the brighter is the region, the higher the Re content is), as observed in arc-melted $(Ru,Re)Si_{1.5}$ polycrystalline alloys in our previous study [11]. The extent of the compositional variation in the chimney-ladder phases observed in directionally solidified alloys is less significant than that observed in arc-melted polycrystalline alloys. While the difference in the Re content of chimney-ladder phases for a given specimen of the Ru-Re-Si ternary system is usually 15-20% for arc-melted polycrystalline alloys, it is only as small as about 5% for directionally solidified alloys.

SEM BSE images of directionally solidified $Ru_{0.27}Re_{0.73}(Si_{1-\delta}Al_\delta)_{1.67}$ quaternary alloys with nominal alloy compositions of δ = 0.04 and 0.08 observed in a cross section cut perpendicular to the growth direction are depicted in Fig. 2. While a secondary monosilicide phase is observed in the alloy with δ = 0.16 (Fig. 2(b)), those with δ = 0.04 and 0.08 contains essentially only the chimney-ladder phases, exhibiting a similar compositional variation (Fig. 2(a)). EDS analysis has indicated a significant loss of Al occurring during crystal growth so that the values of δ decrease from δ = 0.04 and 0.08 (the nominal compositions) to δ = 0.022 and 0.036 (the actual compositions), respectively.

Crystal orientations of columnar grains in directionally solidified ingots inspected by the X-ray Laue back reflection method are found to be nearly parallel to the [001] direction of the tetragonal chimney-ladder phases in all alloys investigated. The orientation difference among adjacent columnar grains are sometimes as large as 15° in the case of Re-poor alloys with the x value smaller than 0.36, while it is at most 2° in the case of Re-rich alloys with the x value greater than 0.53 and Al-containing quaternary alloys. In this perspective, directionally solidified ingots in the latter case can be regarded as single crystals containing some subboundaries.

The values of lattice constants (of the metal subcell) a_M and c_M of the tetragonal chimney-ladder phases in directionally solidified alloys deduced as a function of the Re content by powder X-ray diffraction are tabulated in Table 1, together with the volume of the metal subcell. The value of lattice constants increases monotonously with the increase in the Re content. This is consistent with our previous result obtained for polycrystalline specimens [11].

3.2. TEM analysis

Typical examples of the 00l systematic row in the selected area electron diffraction (SAED) pattern taken along [120] direction of the chimney-ladder phases from various specimens are shown in Fig. 3 in the increasing order of the total electron deficiency per M atom, which corresponds to the Re/(Ru+Re) ratio (x) for the ternary $Ru_{1-x}Re_xSi_y$ chimney-

ladder phases and the sum of the Re/(Ru+Re) ratio and Al/(Si+Al) ratio, i.e. ($x + yz$) for the quaternary $Ru_{1-x}Re_x(Si_{1-z}Al_z)_y$ phases. They are all composed of diffraction spots from the M subcell and those from the X subcell, indicating that the chimney-ladder phases are actually formed in these alloys. According to the method previously described [11], the X/M atomic ratio (y) of the chimney-ladder phases are estimated from the diffraction spots from the M and X subcells, as plotted in Fig. 4 as a function of the total electron deficiency per M atom, which is determined by EDS and WDS analysis in TEM and SEM. As seen from Fig. 4, all directionally solidified ternary alloys possess chemical compositions close to the compositional line determined for arc-melted polycrystalline specimens in our previous study [11]. As in the case of arc-melted polycrystalline specimens [11], the X/M-x_{defect} relation for the $Ru_{1-x}Re_xSi_y$ chimney-ladder phases in directionally solidified alloys deviates from the relation expected from the VEC=14 rule; the X/M values are larger than those expected from the VEC=14 rule for smaller x_{defect} values (smaller Re contents), while the opposite is true for larger x_{defect} values (larger Re contents) with the interception occurring at the x_{defect} value around 0.5. For the Al-containing quaternary $Ru_{1-x}Re_x(Si_{1-z}Al_z)_y$ phases, the extent of deviation of the X/M value from that expected from the VEC=14 rule is larger than that observed for the ternary chimney-ladder phases at a given x_{defect} value. This is exactly what we expected, as discussed in the 4.2 section.

3.3. Thermoelectric properties

Thermoelectric properties of the directionally solidified samples of the ternary $Ru_{1-x}Re_xSi_y$ chimney-ladder phases were measured along their growth direction, i.e. approximately along the [001] direction of the chimney-ladder phases. Since the extent of compositional variation within the chimney-ladder phases is small in directionally solidified ingots when compared to arc-melted polycrystalline ingots, thermoelectric properties characteristic of a given chimney-ladder phase corresponding to a particular alloy composition are expected to be obtained with these directionally solidified ingots.

Values of Seebeck coefficient and electrical resistivity of ternary $Ru_{1-x}Re_xSi_y$ alloys with various x values are plotted in Figs. 5(a) and (b) as a function of temperature. The sign of Seebeck coefficient for Re-poor alloys with the x values smaller than 0.36 is negative in the whole investigated temperature range. In contrast, the sign of Seebeck coefficient for Re-rich alloys with the x values larger than 0.53 is positive in the whole investigated temperature range. The n- and p-type behaviors observed respectively for the Re-poor and Re-rich alloys are consistent with the prediction from the deviation of the X/M-x composition line from the relation expected from the VEC=14 rule (Fig. 4). The p-n transition is thus experimentally confirmed to occur at the composition close to x=0.5, as Fig. 4 predicts. At a given temperature, the absolute values of both Seebeck coefficient and electrical resistivity increase as the extent of the deviation from the VEC=14 rule in Fig. 4 increases, i.e., as the alloy composition deviates from that corresponding to the p-n transition ($x \approx 0.5$). This clearly indicates that the carrier concentration of the chimney-ladder phases is in principle determined by the extent of compositional deviation from the ideal composition corresponding to the VEC=14 rule. The temperature dependence of Seebeck coefficient and electrical resistivity of the $Ru_{1-x}Re_xSi_y$ chimney-ladder phases differ from each other depending on the conduction types (n- or p-types). The absolute value of Seebeck coefficient of all chimney-ladder phases of the n-type ($0.14 \leq x \leq 0.36$) rapidly decreases with the increase in temperature in the range of 100-400K, then gradually increases up to 850 K, followed by a slight decrease above 850 K. The value of electrical resistivity of all these n-type phases first decreases gradually (up to around 850 K) and then rapidly (above 850 K) with the increase in temperature. These indicate that all these n-type chimney-ladder phases

exhibit a typical semiconducting behavior with the intrinsic conduction region above 850K and the extrinsic conduction region below room temperature. In contrast, the absolute value of both Seebeck coefficient and electrical resistivity of all chimney-ladder phases of the p-type ($0.53 \leq x \leq 0.73$) increases monotonously with the increase in temperature, indicating a metallic conduction behavior.

Values of thermal conductivity of ternary $Ru_{1-x}Re_xSi_y$ alloys with various x values are plotted in Fig. 5(c) as a function of temperature. The values of thermal conductivity of ternary $Ru_{1-x}Re_xSi_y$ chimney-ladder phases are quite low when compared to that (5~8 W/m·K) of directionally solidified binary LT-Ru_2Si_3 [9] and they are about 1.25~2.25 W/(m·K) at room temperature. These values tend to increase as the alloy composition deviates from that corresponding to the p-n transition ($x \approx 0.5$), i.e., as the carrier concentration increases. These values of thermal conductivity increase slightly with the increase in temperature. Fig. 5(d) plots values of dimensionless figure of merit (ZT) of ternary $Ru_{1-x}Re_xSi_y$ alloys with various x values as a function of temperature. At a given temperature, the ZT value tends to increase with the increase in the Re content except for the alloys with $x = 0.60$ and 0.73. The ZT value increases with the increase in temperature for all ternary alloys. The maximum value of 0.47 is obtained for the alloy with $x = 0.60$ at 973 K, which is about twice as high as that of directionally solidified binary LT-Ru_2Si_3 [9].

Values of Seebeck coefficient, electrical resistivity, thermal conductivity and dimensionless figure of merit of quaternary $Ru_{0.24}Re_{0.73}(Si_{1-z}Al_z)_{1.67}$ alloys with $z = 0.04$ and 0.08 are plotted in Figs. 6(a)-(d) as a function of temperature together with the corresponding plots for the ternary alloy with $x = 0.73$. Both quaternary alloys containing Al exhibit a similar type of temperature dependence for Seebeck coefficient, electrical resistivity, thermal conductivity and dimensionless figure of merit, although the there are some difference in their absolute values. The values of both electrical resistivity and Seebeck coefficient decrease with increasing the amount of Al substitution, which corresponds well with the increase in the carrier concentration predicted from the extent of compositional deviation from the ideal composition corresponding to the VEC=14 rule. The increase in the carrier concentration is expected to result in the increase in thermal conductivity, however, the value of thermal conductivity decrease with increasing the amount of Al substitution, which suggests that the lattice component of the thermal conductivity decrease with increasing the Al contents. Lattice thermal conductivity (λ_L) for each sample is estimated by subtracting the carrier component, which is approximately calculated using the Wiedemann-Franz law: $\lambda_{carrier} = L\sigma T$, where L is the Lorenz constant ($L = 2.45\times10^{-8}$ WΩ K^{-2}). As indicated with filled marks in Fig. 6(c), the estimated values of lattice thermal conductivity markedly decrease with increasing the amount of Al substitution. Such a decrease in the lattice thermal conductivity is likely to be caused by the lattice disorder introduced by partial substitution of Si with Al. Thus, the Al substitution is found to be very effective in further decreasing the values of electrical resistivity and the lattice component of thermal conductivity of the $Ru_{1-x}Re_xSi_y$ chimney-ladder phases. This results in the improvement of the ZT value up to 0.56 for the alloy with $z = 0.08$ at 973 K.

4. DISCUSSION

4.1. Changes in the thermoelectric properties with alloy composition

As predicted from the compositional deviation from the ideal compositions corresponding to the VEC= 14 rule [22], the thermoelectric properties of the $Ru_{1-x}Re_xSi_y$ chimney-ladder phase are well described qualitatively in terms of changes in the carrier concentration due to the shift of the position of the Fermi energy, which can be estimated from the extent and sign of the composition deviation from the ideal VEC=14 compositions

in the X/M-x_{defect} plot of Fig. 4. We now discuss the changes in the band structure upon substituting Re with Ru in the ternary chimney-ladder phases, with which different types of transport properties observed in n- and p-type chimney-ladder phases (Figs. 5(a) and (b)) are well described. As shown in Fig. 5(b), all n-type chimney-ladder phases exhibit a typical semiconducting behavior, showing an exponential decrease in electrical resistivity with the increase in temperature. For all these n-type chimney-ladder phases, the temperature range above 850 K where a rapid decrease in electrical resistivity with temperature is observed corresponds to the intrinsic region. The activation energies for electrical conduction of the intrinsic region are approximately estimated to be about 0.45eV for the n-type chimney-ladder phases, which is comparable with the value of the band gap (0.44 eV from experiment [24] and 0.34 eV from calculation [7]) previously reported for binary HT-Ru_2Si_3. Since the activation energies are estimated based on the limited numbers of data in relatively narrow temperature range between 850K and 1000K, the values may contain some estimation errors and therefore details of the compositional dependence of the activation energy for the intrinsic region are not discussed in this study. On the other hand, the temperature range below room temperature where a gradual decrease in electrical resistivity with temperature is observed corresponds to the extrinsic conduction region of these n-type chimney-ladder phases with the activation energies depending on alloy composition. They are estimated from Fig. 5(b) to be 0.11, 0.16 and 0.24 eV for the $Ru_{1-x}Re_xSi_y$ alloys with x = 0.14, 0.23 and 0.36, respectively. In view of the fact that the activation energy of 0.24 eV in the extrinsic region for the n-type ternary alloy with x = 0.36 is well in the middle of the band gap of 0.45 eV, the energy band introduced by the substitution of Ru with Re must be degenerated with the valence band and extends widely into the band gap, as illustrated in Figs. 7(a) and (b). In contrast, the conducting behavior of p-type $Ru_{1-x}Re_xSi_y$ chimney-ladder phases with Re-rich compositions is metallic and the value of electrical resistivity decreases with the increase in the Re contents. This implies that the energy band introduced by the Re addition is degenerated with the valence band with the Fermi level being below the top of the valence band (Figs. 7(c) and (d)), as in the case of higher manganese silicides ($MnSi_x$ with $x \sim 1.73$-1.75) [21].

4.2. The compositional deviation from the ideal composition satisfying the VEC=14 rule

The X/M-x_{defect} relation for the $Ru_{1-x}Re_xSi_y$ chimney-ladder phases deviates from the relation expected from the VEC=14 rule so that the X/M values are larger than those expected from the VEC=14 rule for smaller x_{defect} values (smaller Re contents), while the opposite is true for larger x_{defect} values (larger Re contents) with the interception occurring at the x value around 0.5. In addition, the partial substitution of Si with Al, which is larger than Si in atomic radius, is quite effective in increasing the amount of the compositional deviation from the VEC=14 composition, leading to the improved thermoelectric properties.

We now discuss the possible reasons for the systematic compositional deviation in terms of atomic packing. We define the atomic packing factor as the ratio of the volume of atoms located in the unit metal subcell to the volume of the unit metal subcell. The values of the atomic packing factor calculated for the actual compositions of the experimentally observed chimney-ladder phases and the corresponding VEC=14 compositions are shown in Fig. 8 as a function of the Re content. Goldschmidt radii (0.134, 0.138, 0.117 and 0.143 nm respectively for Ru, Re, Si and Al) are used in the calculation. Since the number of valence electrons is smaller for Re (group 7) than Ru (group 8), the X/M ratio of $Ru_{1-x}Re_xSi_y$ chimney-ladder phases is expected to increase with the increase in the Re content as far as the VEC=14 rule is obeyed. Namely, the number of Si atoms in the unit metal subcell has to increase with the increase in the Re content, as shown in Fig. 8. However, the variation of the atomic packing factor for the actual compositions of the experimentally observed chimney-

ladder phases is much smaller than that for the corresponding VEC=14 compositions. This clearly indicates that these chimney-ladder phases can exist with the atomic packing factor in a certain small range and that these phases are destabilized once the atomic packing factor becomes out of the range. Then, these chimney-ladder phases tend to take a X/M ratio within the range of atomic packing factor, which is different from that the VEC=14 rule dictates, so as not to destabilize the crystal structure. This is considered to be the reason for the systematic compositional deviation from the ideal value satisfying the VEC=14 rule. If atomic packing is one of the important factors controlling the stability of chimney-ladder phases, the compositional deviation from the ideal value satisfying the VEC=14 rule should be controlled by alloying additions not only through the difference in the number of valence electrons between Ru and the substitutional element but also through the difference in atomic radius between the two. For example, if Re in $Ru_{1-x}Re_xSi_y$ chimney-ladder phases is partly substituted with a smaller metal atom such as Mn, the volume of the unit metal subcell would become smaller, resulting in the decreased X/M ratio. Similarly, if Si in $Ru_{1-x}Re_xSi_y$ chimney-ladder phases is partly substituted with a larger element such as Ge and Sn, the X/M ratio would also decrease to maintain the range of atomic packing. Then, a large compositional deviation from the corresponding VEC=14 composition is expected to occur when the Re content in p-type $Ru_{1-x}Re_xSi_y$ chimney-ladder phases is large. Since the atomic radius of Al is larger than that of Si, the partial substitution of Si in $Ru_{1-x}Re_xSi_y$ chimney-ladder phases with Al would similarly decreases the X/M ratio, resulting in a large compositional deviation from the corresponding VEC=14 composition when the Re content in p-type $Ru_{1-x}Re_xSi_y$ chimney-ladder phases is large. In addition, since the number of valence electrons is smaller for Al than for Si, the substitution of Si with Al increases the value of electron defects per metal atom (x_{defect} in Fig. 4), also leading to the increase in the amount of compositional deviation from the corresponding VEC=14 composition. Al substitutions in $Ru_{1-x}Re_xSi_y$ chimney-ladder phases are thus expected to be very effective in making the amount of compositional deviation from the corresponding VEC=14 composition of p-type $Ru_{1-x}Re_xSi_y$ chimney-ladder phases larger, thereby in increasing their carrier concentrations. This is indeed experimentally observed in the present study.

5. CONCLUSIONS

(1) The $Ru_{1-x}Re_xSi_y$ chimney-ladder phases in directionally solidified ternary alloys possess chemical compositions close to the compositional line previously determined for arc-melted polycrystalline specimens, exhibiting less compositional variation within the chimney-ladder phases.
(2) The X/M-x_{defect} relation for the $Ru_{1-x}Re_xSi_y$ chimney-ladder phases in these directionally solidified alloys deviates from the relation expected from the VEC=14 rule. The X/M values are larger than those expected from the VEC=14 rule for smaller x_{defect} values (smaller Re contents), while the opposite is true for larger x_{defect} values (larger Re contents) with the interception occurring at the x value around 0.5.
(3) For the Al-containing quaternary $Ru_{1-x}Re_x(Si_{1-z}Al_z)_y$ phases, the extent of deviation of the X/M value from that expected from the VEC=14 rule is larger than that observed for the ternary chimney-ladder phases at a given x value.
(4) The $Ru_{1-x}Re_xSi_y$ chimney-ladder phases exhibit n- and p-type semiconducting behaviors, respectively, at low and high Re concentrations, at which the X/M values are respectively, larger and smaller than those expected from the VEC=14 rule at a given x_{defect} value. At a given temperature, the absolute values of both Seebeck coefficient and electrical resistivity increase as the extent of the deviation from the VEC=14 rule increases, i.e., as the alloy composition deviates from that corresponding to the p-n transition ($x \approx 0.5$), indicating that

the carrier concentration can be controlled by changing the extent of compositional deviation from the ideal composition corresponding to the VEC=14 rule. The highest values of dimensionless figure of merit obtained are 0.47 and 0.56 at 973K for ternary (x = 0.60) and Al-containing quaternary alloys, respectively.
(5) These chimney-ladder phases are considered to exist when the values of atomic packing factor are in a certain small range. Atomic packing is thus considered to be one of the important factors controlling the stability of chimney-ladder phases, which is directly related to the systematic compositional deviation from the ideal value satisfying the VEC = 14 rule for a series of chimney-ladder phases.

ACKNOWLEDGMENTS

This work was supported by Grant-in-Aid for Scientific Research (A) (No. 18206074) and a Grant-in-Aid for Young Scientists (start-up) (No. 20860049) from the Ministry of Education, Culture, Sports, Science and Technology (MEXT), Japan. One (SH) of the authors greatly appreciates the support from Research Fellowships of the Japan Society for the Promotion of Science for Young Scientists.

REFERENCES

1. Vining CB, McCormack JA, Zoltan A, Zoltan LD. AIP Conf Proc 1991; 217: 458.
2. Pecheur P, Toussaint G. Phys Lett A 1991; 160: 193.
3. Vining C.B., AIP Conf Proc 1992; 246: 338.
4. Gottlieb U, Laborde O. Appl Surf Sci 1993; 73: 243.
5. Arita Y, Mitsuda S, Nishi Y, Matsui T, Nagasaki T. J Nucl Mater 2001; 294: 202.
6. Souptel D, Behr G, Ivanenko L, Vinzelberg H, Schumann J. J Cryst Growth 2002; 244: 296.
7. Migas DB, Miglio L, Shaposhnikov VL, Borisenko VE. Phys stat sol (b) 2002; 231: 171.
8. Ivanenko L, Filonov A, Shaposhnikov V, Behr G, Souptel D, Schumann J, Vinzelberg H, Plotnikov A, Borisenko V. Microelectron Eng 2003; 70: 209.
9. Simkin BA, Hayashi Y, Inui H. Intermetallics 2005; 13: 1225.
10. Krivosheev AE, Ivanenko LI, Filonov AB, Shaposhnikov VL, Behr G, Schumann J, Borishenko VE. Semiconductors 2006; 40: 27.
11. Simkin BA, Ishida A, Okamoto NL, Kishida K, Tanaka K, Inui H, Acta Mater 2006; 54: 2857.
12. Inui H, Tanaka K, Kishida K, Harada S. Mater Sci Forum 2007; 561-565: 443.
13. Kishida K, Ishida A, Tanaka K, Inui H. Mater Sci Forum 2007; 561-565: 463.
14. Koyama T, Ishida A, Kishida K, Tanaka K, Inui H. Adv Mater Res 2007; 26-28: 229.
15. Poutcharovsky DJ, Yvon K, Parthé E. J Less-Common Met 1975; 40: 139.
16. Jeitschko W. Parthé E. Acta Cryst 1967; 22: 417.
17. Nowotny H, In: Eyring ER, O'Keefe M, editors. The Chemistry of Extended Defects in Non-Metallic Solids, Amsterdam: North-Holland, 1970, p.223.
18. Pearson WB. Acta Cryst B 1970; 26: 1044.
19. Fredrickson DC, Lee S, Hoffmann R, Lin J. Inorg Chem 2004; 43: 6151.
20. Fredrickson DC, Lee S, Hoffmann R. Inorg Chem 2004; 43: 6159.
21. Migas DB, Shaposhnikov VL, Filonov AB, Borisenko VE, Dorozhkin NN. Phys Rev B 2008; 77: 075205.
22. Imai Y, Watanabe A. Intermetallics 2005; 13: 233.

23. Lu G, Lee S, Lin J, You L, Sun J, Schmidt JT. J Solid State Chem 2002; 164: 210.
24. Susz CP, Muller J, Yvon K, Parthé E. J Less-Common Met 1980; 71: P1.

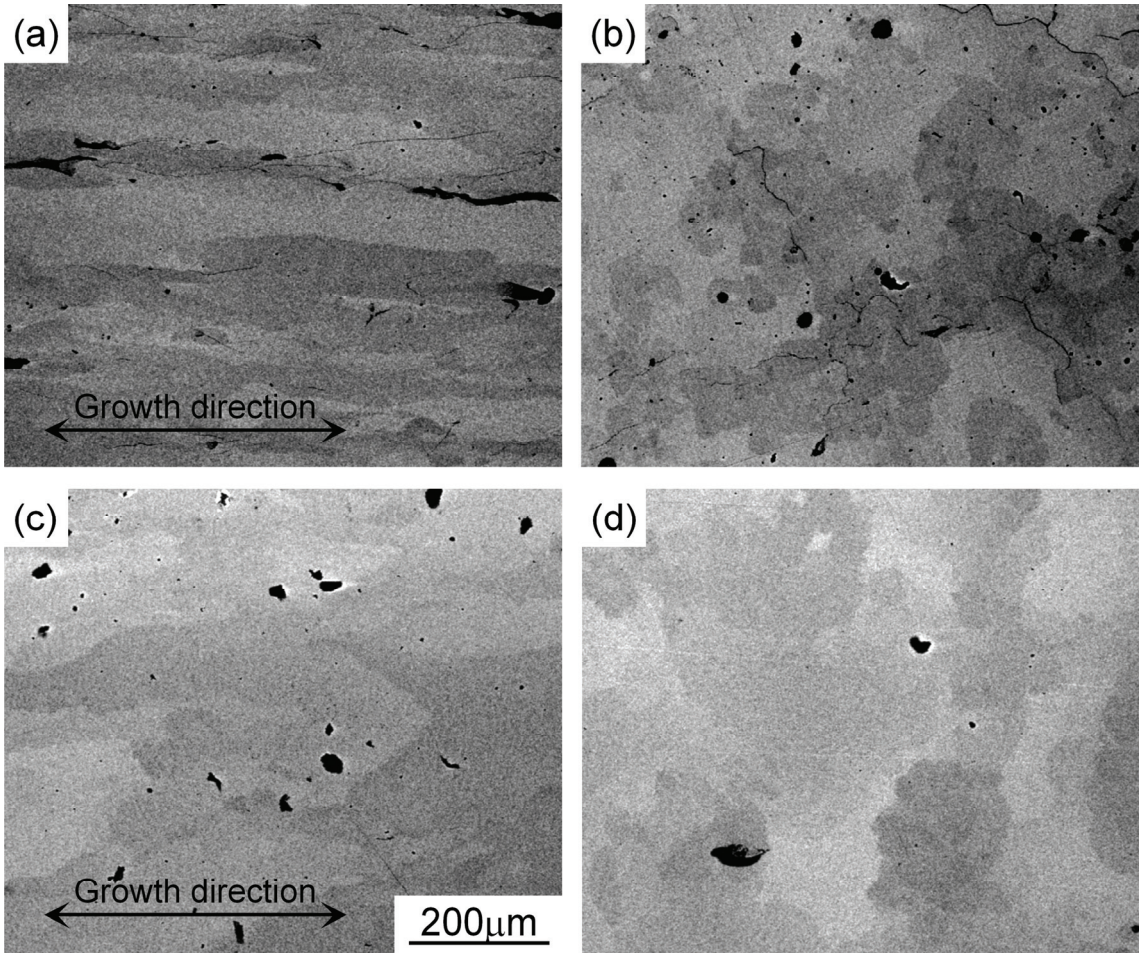

Fig. 1. SEM backscattered electron images of directionally solidified $Ru_{1-x}Re_xSi_{1.54+0.18x}$ ternary alloys with nominal compositions of (a), (b) $x = 0.36$ and (c), (d) $x = 0.60$ observed in a cross section cut (a), (c) parallel and (b), (d)perpendicular to the growth direction.

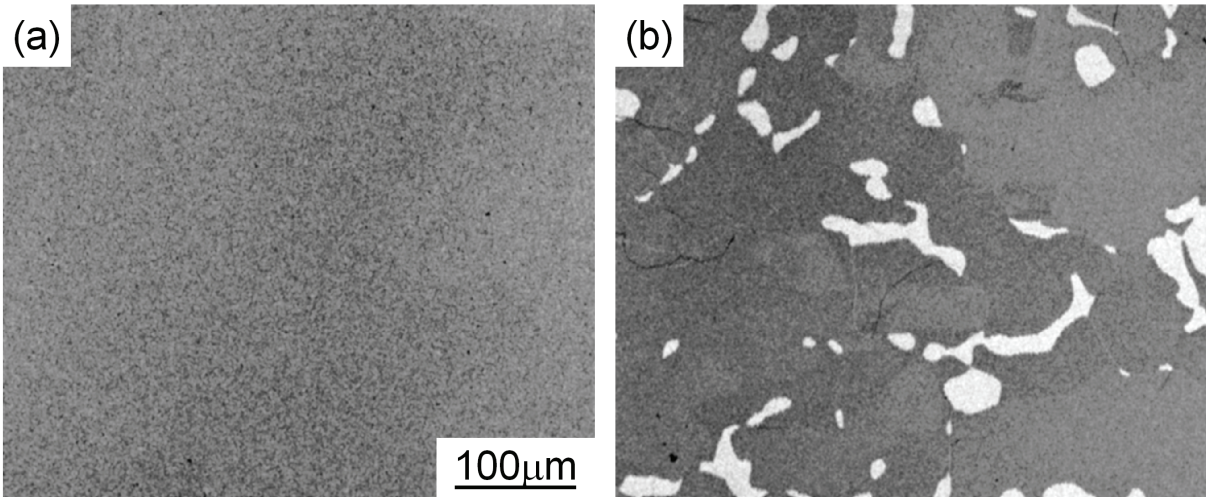

Fig. 2. SEM backscattered electron images of directionally solidified $Ru_{0.27}Re_{0.73}(Si_{1-\delta}Al_\delta)_{1.67}$ quaternary alloys with nominal compositions of (a) $\delta = 0.04$ and (b) 0.08 observed in a cross section cut perpendicular to the growth direction.

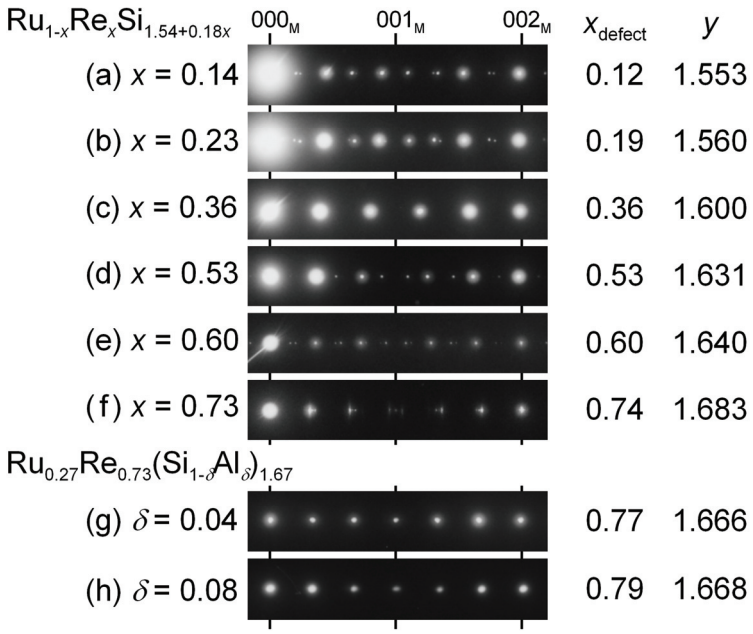

Fig. 3. Typical examples of the 00*l* systematic row in SAED patterns taken along [120] direction of the chimney ladder phases from various directionally solidified alloys. These are shown in the increasing order of the total electron deficiency per M atom, which corresponds to the Re/(Ru+Re) ratio (x) for the ternary $Ru_{1-x}Re_xSi_y$ chimney-ladder phases and the sum of the Re/(Ru+Re) ratio and Al/(Si+Al) ratio, i.e. ($x + yz$) for the quaternary $Ru_{1-x}Re_x(Si_{1-z}Al_z)_y$ phases.

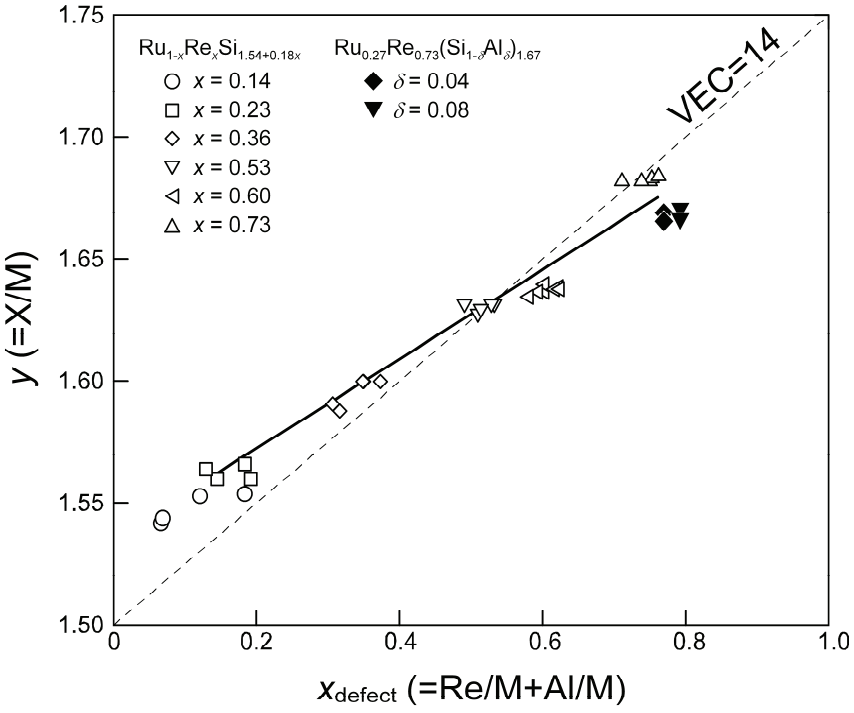

Fig. 4. X/M ratio for the $Ru_{1-x}Re_xSi_y$ and $Ru_{0.27}$ $Re_{0.73}(Si_{1-z}Al_z)_y$ chimney-ladder phases plotted against electron defects per metal atom (x_{defect}). The X/M-x compositional line determined for arc-melted polycrystalline specimens in our previous study [11] is indicated with a thick line, while that expected from the VEC=14 rule is indicated with a broken line.

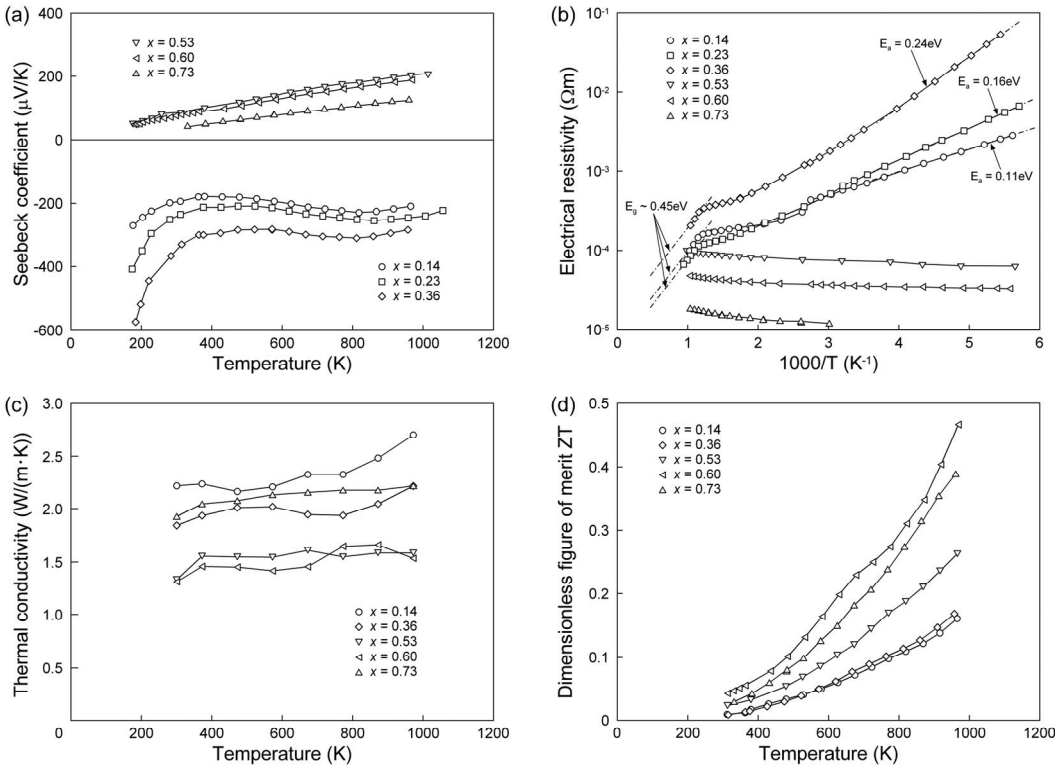

Fig. 5. Values of (a) Seebeck coefficient, (b) electrical resistivity, (c) thermal conductivity and (d) dimensionless figure of merit of ternary $Ru_{1-x}Re_xSi_y$ alloys with various x values plotted as a function of temperature.

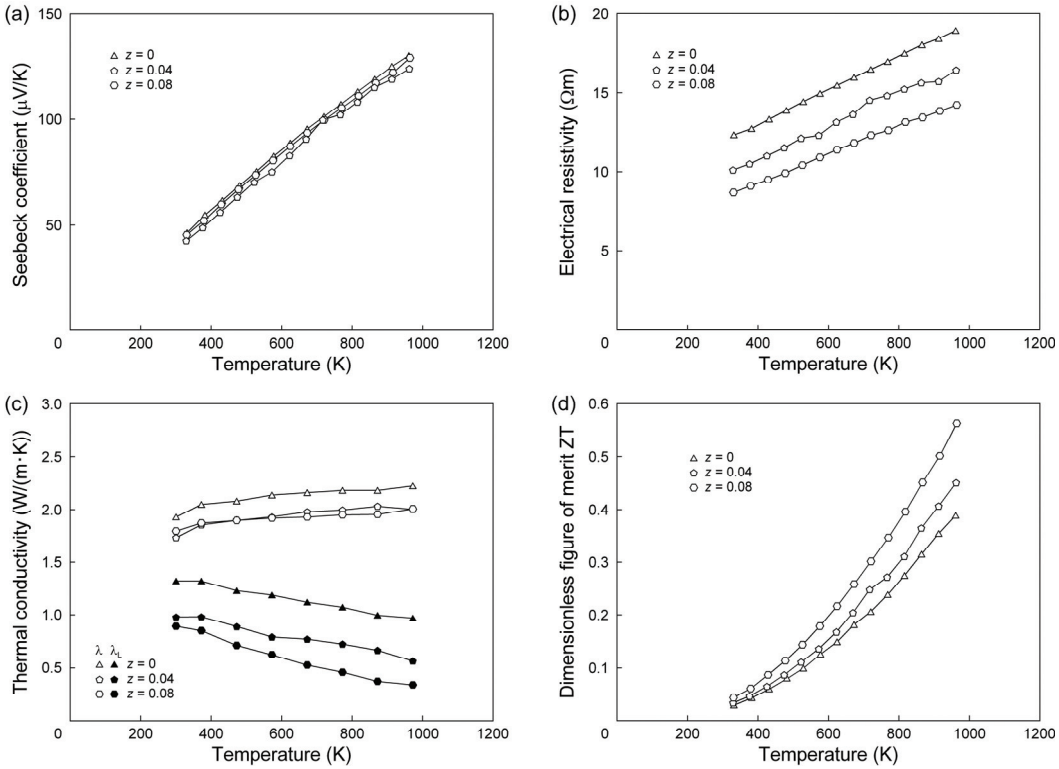

Fig. 6. Values of (a) Seebeck coefficient, (b) electrical resistivity, (c) thermal conductivity and (d) dimensionless figure of merit of quaternary $Ru_{0.24}Re_{0.73}(Si_{1-z}Al_z)_{1.67}$ alloys with z = 0.04 and 0.08 plotted as a function of temperature. The corresponding plots for the ternary alloy with x = 0.73 are also shown.

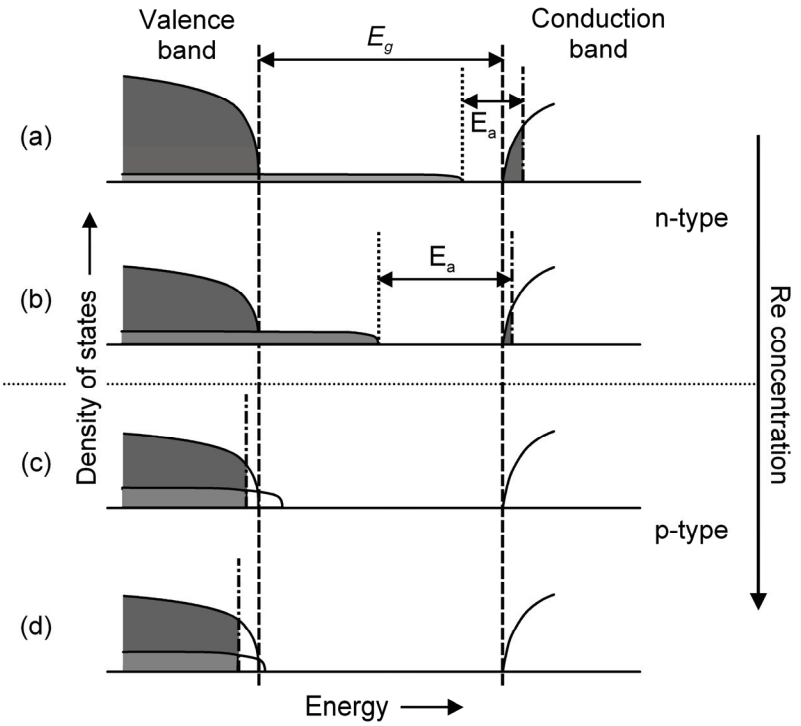

Fig. 7. Schematic illustration of changes in the band structure upon substituting Ru in $Ru_{1-x}Re_xSi_y$ chimney-ladder phases with Re. (a) (b) n-type and (c) (d) p-type.

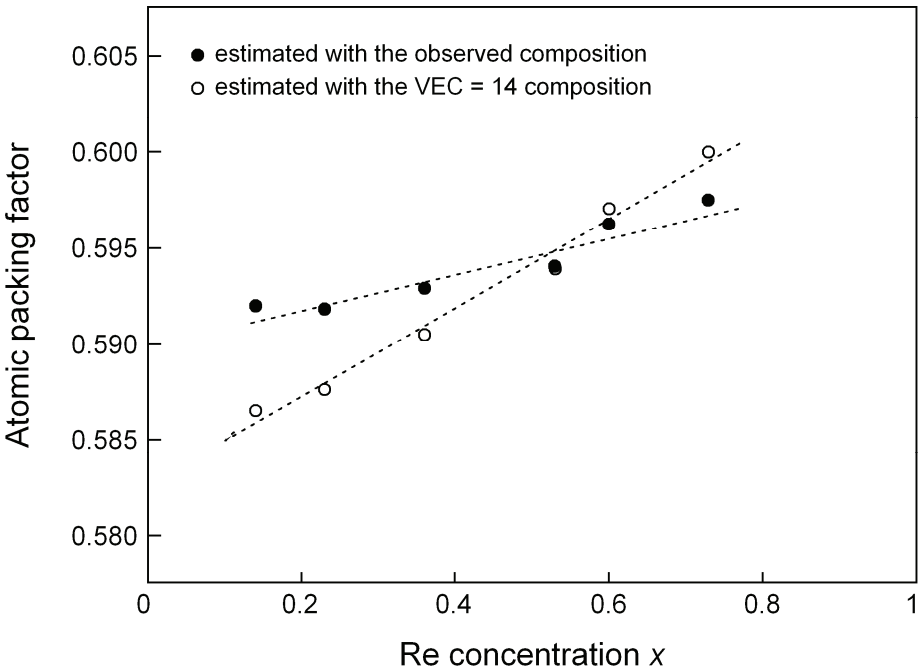

Fig. 8. The values of the atomic packing factors calculated for the actual compositions of the experimentally observed chimney ladder phases and the corresponding VEC=14 compositions are shown in Fig. 8 as a function of the Re content. Goldschmidt radii (0.134, 0.138, 0.117 and 0.143 nm respectively for Ru, Re, Si and Al) are used in the calculation.

Table 1. Crystallographic parameters for ternary $Ru_{1-x}Re_xSi_y$ chimney-ladder phases with various chemical compositions.

Re/M ratio x	Lattice constants for the metal sublattice		A unit volume of the metal subcell V_M	Distance between adjacent metal atoms	Angle between two metal-metal bonds	Atomic packing factor (Exp.)	Atomic packing factor (VEC =14)
	a_M	c_M					
0.14	0.5601	0.4458	0.1399	0.3014	136.60	0.5920	0.5866
0.23	0.5629	0.4457	0.1412	0.3027	136.80	0.5919	0.5877
0.36	0.5654	0.4467	0.1428	0.3039	136.88	0.5929	0.5905
0.53	0.5685	0.4485	0.1450	0.3056	136.95	0.5941	0.5940
0.60	0.5691	0.4490	0.1454	0.3059	136.94	0.5963	0.5971
0.73	0.5712	0.4504	0.1470	0.3070	136.96	0.5975	0.6000